JCSE The Journal of Corrosion Science and Engineering
ISSN 1466-8858 Volume 15, Preprint 8 submitted 18 January 2012

Metastable Pitting Corrosion in 316LN Stainless Steel Using Electrochemical Noise Analysis

M.G. Pujar* and U. Kamachi Mudali

Corrosion Science and Technology Group (CSTG)
Indira Gandhi Centre for Atomic Research (IGCAR)
Kalpakkam – 603 102, India.

* Corresponding author: pujar@igcar.gov.in

Phone: +91 44 27480121

Fax: +91 44 27480121

Abstract

The growth and decay of the metastable pitting was studied using electrochemical noise (EN) signals collected after 5th, 12th and 19th day of immersion of Type 316LN stainless steel (SS) specimens in 0.5M Sodium chloride solution. EN data was processed using Weibull distribution function to know the mean-free time for pit initiation. Metastable pit radii as well as maximum metastable pit radii (Pit_{max}) were calculated using Gumbel distribution. The results indicated that the mean-free time values for pit initiation increased and Pit_{max} decreased with increase in the time of immersion suggesting the role of nitrogen in repassivation of the pits.

Key words: Stainless steel, Electrochemical Noise, Pitting corrosion, Weibull distribution, Gumbel distribution, Maximum pit depth

Introduction

It is important to have an effective localized corrosion damage prediction methodology in order to successfully avoid the unpredicted corrosion failures and consequent unscheduled downtime in industrial systems and for the successful implementation of life extension strategies [1]. Majority of the chemical plant failures are attributed to the localized corrosion like pitting. A large number of pits are formed on stainless steels when they are exposed to chloride containing environment. However, the vast majority of these pits only grow for a very short time and to a small depth known as metastable pits [2, 3]. Some pits however, become stable and continue to grow for longer periods of time and to much greater depths [2, 3]; it is these stable pits that are important when considering their effects on corrosion damage and failure. Stable pits and metastable pits are thought to be initiated in the same manner and stable pits are considered to be a subset of the metastable pits [2]. Each pit produces a small spike in the electrical current of a few seconds duration, indicating an anodic reaction and the spike then dies out, which indicates the formation and repassivation of a microscopic metastable pit. Experimental and theoretical studies have largely clarified the mechanism for the

JCSE The Journal of Corrosion Science and Engineering
ISSN 1466-8858 Volume 15, Preprint 8 submitted 18 January 2012

initiation of these microscopic pits as being caused by localized electrodissolution of metal at surface defects and inclusions [4-7]. Unlike stable pits, metastable pits only grow to a very small size at which stage their propagation is arrested from further growth [8]. In light of the reactivity of the metal the only possible reason for these pits to cease from growing is the regeneration of protective oxide coating. In order to predict when stable pits will develop it is therefore important to determine when metastable pitting occurs, and subsequently the likelihood of these metastable pits becoming stable pits. The study of metastable pitting is therefore a key in the prediction of the development of pitting corrosion [9] and the damage caused thereof leading to failures.

Type 316LN Austenitic Stainless Steel is the structural material for the Prototype Fast Breeder Reactor (PFBR) being built at Kalpakkam, India. It is being used in many structural components of PFBR such as main vessel, safety vessel, inner vessel, auxiliary grid plate, fuel transfer machines, intermediate heat exchangers and core support structures because of its adequate strength, corrosion resistance, good weldability and compatibility with liquid sodium. Low carbon grades have been chosen to ensure freedom from sensitization during welding of the components and to avoid the risk of chloride stress corrosion cracking during storage in coastal site of Kalpakkam. Since low carbon grades have lower strength than normal grades, nitrogen is specified as an alloying element to improve the mechanical properties so that the strength is comparable to 316 SS. However, several austenitic steels suffer extensive pitting or localized corrosion in the presence of halide ions. Since, as stated earlier, the metastable pits are the precursors to the stable pits, it is important to analyze the formation, growth and decay of the metastable pits. In the present investigation EN technique was used to study the metastable pitting process on 316LN SS, as analysis of EN signals generated during metastable pitting can also provide details about the initiation, propagation and repassivation process of this state. The progress of the metastable pits was studied by exposing 316LN SS specimens to aerated 0.5M sodium chloride solution for about 20 days; the EN data analysis was conducted using Weibull and Gumbel distribution functions.

Experimental procedure

The chemical composition of the 316LN SS is given in Table 1.

Table 1: Chemical composition of 316LN SS, wt. %

Element	C	Cr	Ni	Mo	N	Mn	Si	P	S	Ti	Nb	Cu
Wt.%	0.025	18.16	11.90	2.4	0.067	1.62	0.28	0.044	0.01	0.019	0.032	0.560

Generally, the specimens for corrosion tests are mounted in Araldite resin with an electrical contact for external connection in order to polish the flat surface with ease. However, this conventional arrangement has shown to be deleterious as far as localized corrosion studies are concerned since, the gap between the specimen and the resin acts as a crevice and erroneous results are obtained. Therefore, cylindrical specimens were used in our experiments so as to avoid mounting them into Araldite resin and subsequent crevice attack. The cylindrical specimens (25 mm length, 10 mm dia.) were drilled and tapped at one end in order to establish electrical contact with the electrochemical measurement system using a specimen holder rod. These specimens were polished up to fine diamond (1 μm) on the curved surface and ground to 1200 grit on the flat surfaces. The sharp edges at the boundary of the curved surface and the flat surface were rounded off to avoid preferential attack. The specimens were washed in soap solution and cleaned ultrasonically in methanol and dried before

JCSE The Journal of Corrosion Science and Engineering
ISSN 1466-8858 Volume 15, Preprint 8 submitted 18 January 2012

immersing in the solution. The specimens prepared in this manner were used in our studies. These specimens were partially immersed in the solution, the specimen holder rods holding the cylindrical specimen were covered with Teflon tape and were out of the solution. Since only the flat surface of a cylindrical specimen was immersed in the solution, the area exposed to the solution was 0.767 cm^2. The anodic polarization experiments were performed in five-necked polarization cell with a luggin-haber probe and a salt-bridge in order to establish the contact of the working electrode with the reference electrode. All solutions were prepared using double-distilled water. All the experiments were performed in the aerated solution of sodium chloride; sodium chloride of analytical reagent grade was used for the experiments. The potentials were measured against saturated calomel electrode (SCE). Two platinum foils (with an area of 1 cm^2 each) spot-welded to the platinum wires were used as the counter electrodes and were placed symmetrically on the opposite sides of the working electrode. The scan rate was chosen to be 0.1667 mV/s. Initially, the specimen was immersed in the solution for 45 min in order to observe the stable open circuit potential (OCP). Thereafter, anodic polarization was carried out from cathodic region (–250 mV(SCE)) until the current rise was monotonic indicating the initiation of the stable pitting corrosion. The anodic polarization curves with high noise at lower current densities were corrected using a smoothening function. Basically these are the filters which are used to remove the noise from the data file. These methods are based on the Savitzky Golay (SG) smoothening method. In effect, a sequence of data points was fitted to a cubic equation and a new value for each point is calculated from the cubic equation. The level of smoothening is controlled by the number of points used in the fitting process. Thus, the polarization diagram was smoothened removing high noise in the low current regime. The B (Stern-Geary coefficient) value was determined from that region of the anodic polarization curve which represented the stable pitting, as per the procedure given by Na et al. [10].

Electrochemical Noise Studies

Electrochemical noise studies on this material were performed using two nominally identical cylindrical specimens with the same chemical composition as well as metallurgical history. The specimens were connected to the EN measurement system (Solartron SI 1287 with current and potential sensitivities as low as 1 pA and 1 µV respectively) using threaded specimen rods, which were covered with Teflon tape. The specimens were polished up to 1200 grit finish, washed in soap water and degreased and ultrasonically cleaned in methanol. Potential and current noise measurements were performed by short-circuiting together two identical working electrodes. The current flowing between the two working electrodes, as well as the potential between the working electrode and a reference electrode were monitored. The area of the specimen exposed to the solution was about 1.534 cm^2. The potentiostat, which can perform this experiment actively, holds the working electrode connection at the ground potential by a small amplifier circuit. If one working electrode is directly connected to ground and the other is connected to the working electrode cable, they are both held at the same potential and are, in effect, short-circuited together. Any current, which flows between the two electrodes, is measured by current measurement circuits thus creating a Zero Resistance Ammeter (ZRA). The potential is measured between the working electrodes (since they are short-circuited together, both working electrodes are at the same potential) and a reference electrode. SCE was used as a reference electrode for the measurement of potential noise.

Localized corrosion events are frequently characterized by large amplitude corrosion events such as metastable pitting, which have relatively low frequency. The current and potential fluctuations are usually less than a µA and a µV respectively and are of low amplitude and frequency (1 Hz or

less); the factual and meaningful frequency window for the corrosion processes falls in the range of 1 mHz to 1 Hz [11]. Similarly, Cottis [12] showed that the shot-noise parameters f_n and q diverge when the sampling frequency (thereby the frequency bandwidth) exceeds 1 Hz. Electrochemical current and potential noise studies were conducted in aerated 0.5M Sodium chloride solution at OCP and noise signals were collected at the sampling frequency of 1 Hz. Since in EN studies the signal is mostly non-stationary, the drift or the trend gets introduced. Therefore, the drift or the trend removal was carried out using a suitable detrending technique, which is an accepted practice, before calculating the statistical parameters as well as power spectral density (PSD) values. All the potential and current noise data collected in the time domain were transformed in the frequency domain through the fast Fourier transform (FFT) method, by a dedicated software after suitably detrending. FFT based measurements are subject to errors from an effect known as leakage. This effect occurs when the FFT is computed from of a block of data which is not periodic. To correct this problem appropriate windowing function must be applied. If windowing is not applied correctly, errors may be introduced in the FFT amplitude, frequency or overall shape of the spectrum. Since most signals are not periodic in the predefined data block time periods, a window must be applied to correct for leakage. A window is shaped so that it is exactly zero at the beginning and end of the data block and has some special shape in between. This function is then multiplied with the time data block forcing the signal to be periodic. Thus, in order to reduce the leakage of the low as well as the high frequencies in the calculated PSD values, Hanning window was used for signal analysis.

Data analysis using stochastic theory and shot noise

Usually a large scatter is observed in the measurable parameters like corrosion rate, maximum pit depth, time to perforation etc. during localized corrosion. This scatter results from the influence of metal surface heterogeneities and from variations in the corrosive environment over time during pit growth. All these facts suggest that randomness is an inherent and unavoidable characteristic of pitting corrosion as a function of time, so that stochastic models are better suited to describe pitting corrosion process. The output obtained using the stochastic models is random or probabilistic. It may be possible to predict the generation probability of events in the future from the past events, which is termed as, “conditional probability” [13].

Shot noise theory is based on the assumption that the current signal is composed of discrete charge carriers [14]. Shot noise is produced when the current takes the form of a series of statistically independent packets of charge, with each packet having a short duration [15]. The number of charge carriers passing a given point will be a random variable. According to the stochastic process the individual events are independent of other events, thus, shot noise analysis is applicable to the individual events [14, 15]. This theory can be applied to the analysis of electrochemical noise data from corrosion processes. If this theory is applied to EN, three parameters can be obtained: I_{corr} the average corrosion current, q the average charge (also called as characteristic charge) in each corrosion event, and f_n frequency of the appearance of these events. Only two of these parameters are independent, since

$$I_{corr} = q * f_n \qquad (1)$$

it is not possible to measure I_{corr}, q and f_n directly, but it is possible to estimate them from the measured current and potential noise [16]. Assuming that shot noise is produced during breakdown of the passive film as well as pit initiation and hydrogen evolution, the q and f_n are given as [17]:

$$q = \frac{\sqrt{PSD_E * PSD_I}}{B} \quad \text{and} \quad q = \frac{\sigma_I \sigma_E}{Bb} \qquad (2)$$

$$f_n = \frac{B^2}{PSD_E * A} \quad \text{and} \quad f_n = \frac{B^2 b}{\sigma_E^2} \qquad (3)$$

where PSD_E and PSD_I are the low frequency PSD values of the potential and current noise respectively, σ_I and σ_E are the standard deviation values of current and potential respectively and b is the bandwidth of measurement as, standard deviation is a function of measurement bandwidth and A is the surface area of the specimen. The charge q is independent of area and f_n is proportional to area, so it can be reported as events per second per unit area [16]. In these calculations the B value was not taken to be 0.026 V as reported earlier [15]; B value was determined from the potentiodynamic anodic polarization curve, as it is found to be somewhat different than 0.026 V.

The cumulative probability $F(f_n)$ at each f_n is determined from the set of f_n values calculated using equation 3 given above according to the mean rank approximation [14]. According to this method (using f_n as an example): 1) all the values of f_n were sorted in an ascending order and 2) then the cumulative probability for each value was calculated as n/(N+1), where n is the position in the sorted list, and N is the total number of entries in the list [14]. Similarly, the characteristic charge, q values were calculated as per the equation 2 and cumulative probability F(q) was calculated at each q value.

Pit initiation time will follow a Weibull distribution [18] when it is regarded as the survival time defined as the time to first failure (passive film breakdown) of an individual part or process. Following this reasoning, the Weibull distribution is assumed as the distribution of the pit initiation times. Weibull distribution function is one of the frequently used cumulative probability functions for predicting life time in reliability test [13]. Using this distribution it is possible to analyze data even when two or more failure modes are present at the same time [19]. The Weibull distribution is often used in the field of life data analysis due to its flexibility—it can mimic the behavior of other statistical distributions such as the normal and the exponential by modifying m parameter value as shown below. The cumulative probability F(t) of a failure system can be written just as Weibull distribution function, which is expressed as [13],

$$F(t) = 1 - \exp(-t^m / n) \qquad (4)$$

m and n are the shape and scale parameters, respectively; m is a dimensionless parameter and n is expressed as s^m. The Weibull distribution has a relatively simple distributional form. However, the shape parameter allows the Weibull to assume a wide variety of shapes, depending on the value of the shape parameter. The effect of the scale parameter is to stretch out the graph. The equation 4 can be rewritten as follows:

$$\ln\{\ln[1/(1-F(t))]\} = m \ln t - \ln n \qquad (5)$$

By using the cumulative probability values for the localized corrosion events, f_n calculated previously, in the above equation and fitting, two parameters m and n can be determined from the slope of the linear plot of ln{ln[1/(1-F(t))]} versus ln t, (also known as Weibull probability plot) and from the intercept on the ln{ln[1/(1-F(t))]} axis, respectively. The pit nuclei or embryo generation rate is defined as,

$$r(t) = \frac{m}{n} t^{m-1} \qquad (6)$$

based upon Weibull distribution function.

JCSE The Journal of Corrosion Science and Engineering
ISSN 1466-8858 Volume 15, Preprint 8 submitted 18 January 2012

In order to study the progress of metastable pitting or passivation in 316LN using Weibull probability plots, 100 data sets each consisting of 1024 EN data points recorded on 5th, 12th and 19th days after immersion were used. This was done in order to study the progress in the metastable pitting corrosion rate. These EN data points from these 100 data sets were detrended using linear detrending technique to calculate the shot-noise parameters given by equations 2 and 3. Subsequently, Weibull probability plots were constructed to determine the mean-free time values for pit initiation.

Extreme value statistical analysis

Extreme value analysis enables prediction of the most probable maximum extent of corrosion, for example, the deepest pit in the case of the pitting corrosion. It was Gumbel who suggested that extreme-value statistics might be applied to predict the maximum depth of a pit in soil [20, 21]; and Aziz actually showed that the extreme-value theory could be applied to analyze the maximum pit depth of aluminum alloys [22]. Shibata et al. [23], estimated the maximum pit depth on a large oil tank base plate using the extreme-value analysis by sampling small number of specimens with a small area. Pit depth extreme values have been shown to follow the Gumbel distribution for maxima [24-27]. In the present investigation too, Gumbel extreme value distribution was used to model the behaviour of the deepest pits.

When probability of a random variable x follows a doubly exponential distribution of the maximum values (first order asymptotic distribution), the corresponding cumulative distribution function $F_1(x)$ can be expressed as,

$$F_1(x) = \exp\left[-e^{-(x-\mu)/\alpha}\right]; \quad -\infty < x < \infty \qquad (7)$$

where μ is the location parameter and α is the scale parameter [27]. The μ and the α values are the average and the standard deviation of the random variable which describe the centre and the shape of the probability distribution of the maximum metastable pit radii [9]. The integration of current signal with time was used to determine the charge passed for each current transient. This charge is the result of the formation of a single metastable pit that can be related to its physical volume by using Faraday's equation given below,

$$Pit\ Volume\ (cm^3) = \frac{Charge\ Passed\ *\ molecular\ mass}{Faraday\ Constant\ *\ n\ *\ Density} \qquad (8)$$

$$Pit\ radius\ (\mu m) = \left(\sqrt[3]{\frac{3\ *\ volume\ (cm^3)}{2\pi}}\right) * 10{,}000 \qquad (9)$$

where, n is the number of electrons transferred in an anodic reaction and volume in equation 9 refers to the pit volume calculated using equation 8. It is assumed that this charge is not supplemented by charge from the hydrogen reduction reaction within the pit. This assumption was based on the correlation between optically observed metastable pit sizes and the anodic current transient charge values reported by Pride et al. [8]. The 100 current EN data sets collected on 5th, 12th and 19th days were used for extreme-value analysis. If the pits are assumed to be hemispherical the pit radii could be calculated using equation 9 given above. The integrated charges associated with the largest current transients from each data set were used to calculate the pit radii. First, all the calculated extreme values of the pit radii were arranged in the descending order and then the cumulative probability F(Y) was calculated as 1– [M/(N+1)), where M is the rank of the ordered pit radii calculated using extreme values and N is the total number of the pit radii. The reduced variate (Y) can then be calculated by using formula Y = –ln{–ln[F(Y)]} [8-9, 22-27]. From the distribution parameters (μ and α) the values

JCSE The Journal of Corrosion Science and Engineering
ISSN 1466-8858 Volume 15, Preprint 8 submitted 18 January 2012

of the largest expected pit and probability of a pit of a given size were calculated using the following equations,

T = A/a and $Pit_{\max} = \mu + \alpha \ln T$ 10)

Probability of Pit size = $\exp\left\{-\exp\left[\frac{-\left(R_{pit} - [\mu + \alpha \ln T]\right)}{\alpha}\right]\right\}$ 11)

Where "A" is equal to the area over which a prediction is to be made and "a" is the area of the small specimens used in the laboratory to establish the distribution parameters. In the present investigation T was assumed to be 1. Using parameters μ and α it is possible to calculate the largest expected pit size and the probability of a pit of a given size using equation 11 [23]. Specifically, the Gumbel Type I extreme-value distribution is used for extrapolating the corrosion damage measured on a series of small specimens of area "a" to a large system (for example, tanks or pipe lines) with area, "A" [24].

Results and discussion

The potentiodynamic anodic polarization diagram for 316LN SS in 0.5M sodium chloride solution is shown in Fig.1.

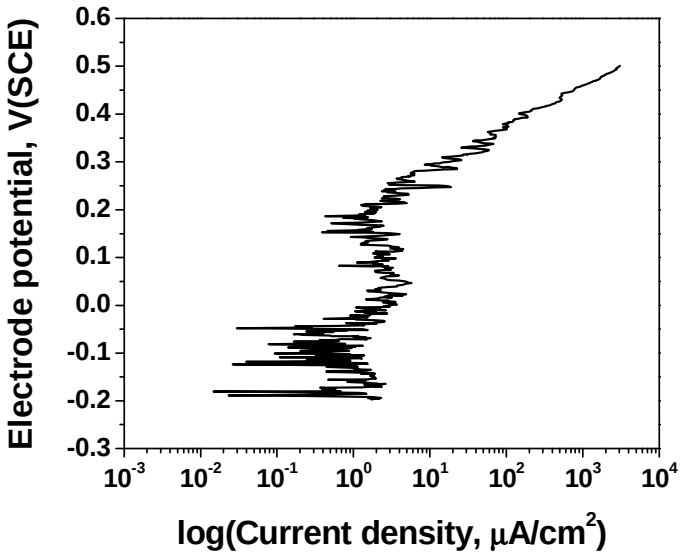

Fig.1	The potentiodynamic anodic polarization diagram for 316LN SS obtained in aerated 0.5M sodium chloride solution

Since the sodium chloride solution is open to air, the cathodic reaction being mass-transport limited oxygen reduction, cathodic Tafel slope is infinity therefore, Stern-Geary coefficient B becomes $B = \frac{\beta_a}{2.303 \times 1000}$. Thus, knowing anodic Tafel slope one can obtain B value. From the potentiodynamic polarization curve (Fig.1), the anodic Tafel slope was determined (in the metastable pitting region which was noted to be 0.25 to 0.35 V(SCE)) to be 65.274 mV/decade; thus, the B value was calculated to be 0.0283 V; this value was used throughout all the calculations using formulae given in equations 2 and 3. Some important visual records of the correlated current and potential EN

JCSE The Journal of Corrosion Science and Engineering
ISSN 1466-8858 Volume 15, Preprint 8 submitted 18 January 2012

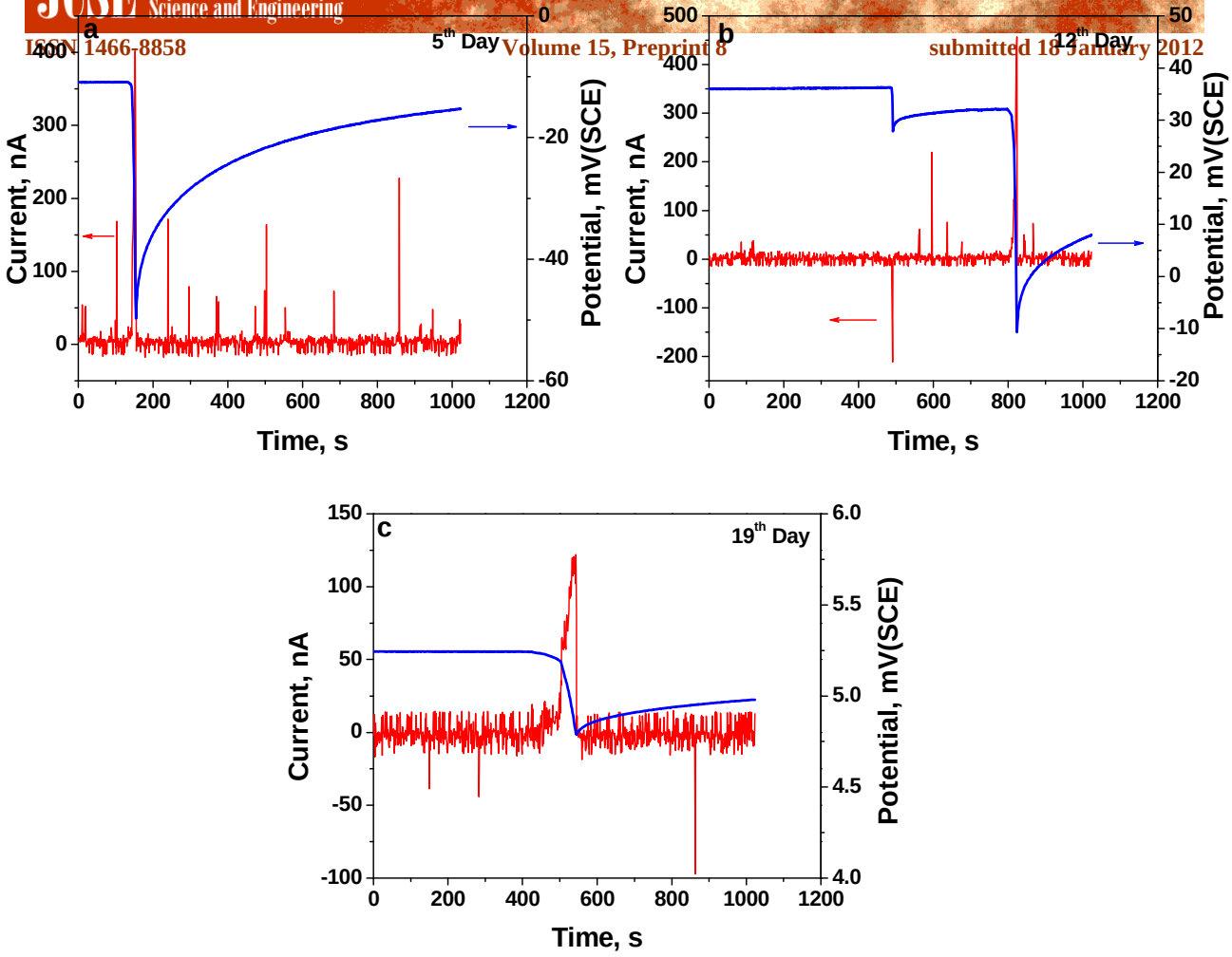

Fig.2 The current and potential EN records for 316LN SS obtained after immersion of (a) 5 days, (b) 12 days and (c) 19 days in aerated 0.5M sodium chloride solution

signals recorded for 1024s are shown for 316LN SS after immersion in the 0.5M Sodium chloride solution for 5, 12 and 19 days (Fig.2 (a-c)); these records show some important EN signatures indicating the behavior of the material in sodium chloride solution.

It was observed that after the exposure of 5 and 12 days the indication of the specimen undergoing metastable pitting was obvious through the current and potential signals, as in both these records there was a sudden drop in the potential signal with a concurrent rise in the current signal, thus, it was clear that the specimen was undergoing metastable pitting. The visual record after 19 days too showed that the process of metastable pitting was still underway; however, the smaller amplitudes of the current and potential signals indicated that the onset of passivation process had begun.

The Weibull probability plots for 316LN in as-received condition are shown in Fig.3 (a, b); the plots were prepared using PSD values as well as standard deviation values according to the equations 2 and 3. The data in these plots could be fitted to two straight lines satisfactorily. In an earlier work [13, 28], it was reported that the slopes in the relatively lower $1/f_n$ region were associated with the

JCSE The Journal of Corrosion Science and Engineering
ISSN 1466-8858 Volume 15, Preprint 8 submitted 18 January 2012

dominant uniform corrosion (in the passive state) or passivation, whereas the slopes in the relatively longer $1/f_n$ region were associated with the dominant pitting corrosion for the latter was a slow process. This method was found to be useful in distinguishing the pitting corrosion events from the passivation events in a practical way [13, 27]. Since the space of the distribution function should be

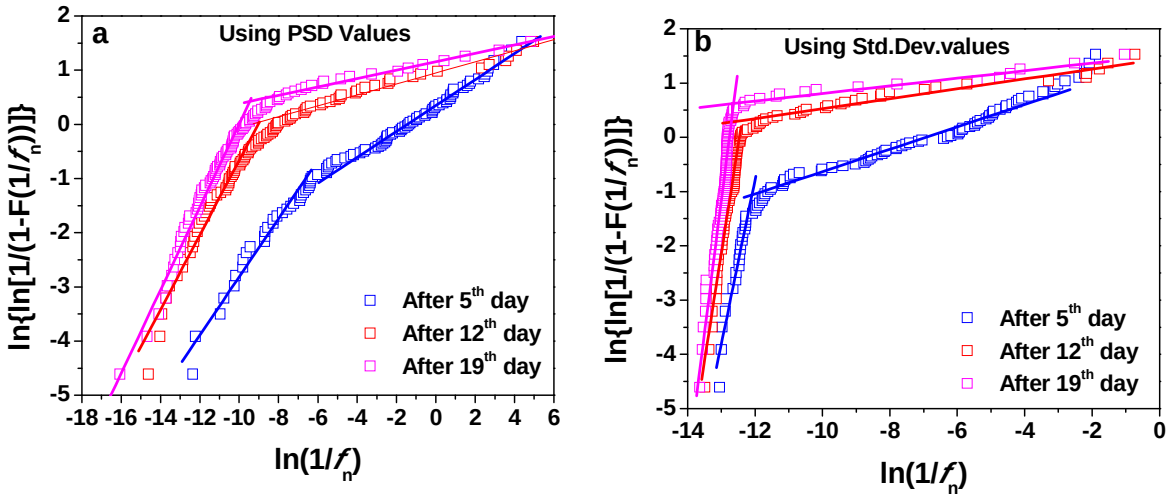

Fig.3 The Weibull Probability plots for 316LN in as-received condition using (a) PSD values and (b) standard deviation values; at different time intervals

the positive time axis, the plots of the cumulative probability were transformed from the f_n domain to the $1/f_n$ mean-free time domain before applying the Weibull distribution function to $F(1/f_n)$. This was done in order to investigate the slow events associated with dominant pitting corrosion in more detail according to the stochastic theory [10]. The intersection point of the two straight lines gives the mean-free time of the initiation of pitting corrosion. Thus, it could be inferred from Fig.3 (a, b) that pitting corrosion was already initiated after the immersion of the specimens for five days. However, it was clear that the pit initiation process slowed down with increase in the exposure time. The mean-free time values for pit initiation are given Table 2.

Table 2: Mean-free time for pit initiation in aerated 0.5M Sodium chloride

Exposure period, d	Mean-free time using PSD values, s	Mean-free time using standard deviation values, s
5	7.7278×10^{-5}	3.2960×10^{-6}
12	1.3082×10^{-4}	4.3000×10^{-6}
19	8.2362×10^{-4}	5.6283×10^{-6}

It was noted that the mean-free time for initiation of pitting increased with increase in the immersion time of the material. The correlation coefficient between the values obtained by using PSD as well as standard deviation values was 0.93, indicating an excellent correlation. The shape parameter (m) and the scale parameter (n) values were obtained by linearly fitting the data points in the Weibull probability plots (Table 3). It was noted that both m and n decreased continuously as a function of exposure time. It was reported by Dey et al., [29] that the continuous increase in the scale parameter

JCSE The Journal of Corrosion Science and Engineering
ISSN 1466-8858 Volume 15, Preprint 8 submitted 18 January 2012

was a reflection of the decrease in the proportion of small-sized pits with increasing exposure. However, in the present condition this does not seem to be the case as can be seen later. Pit embryo generation rates were calculated by inserting the values of these parameters in equation 6 at different exposure times. The plots of the pit embryo generation rates as a function of time are shown in Fig.4.

Table 3: Weibull distribution parameters for the 316LN SS at different exposure Times in aerated 0.5M sodium chloride solution

Exposure time, d	316LN SS	
	Shape parameter m (-)	Scale parameter n (s^m)
5	0.239	0.705
12	0.102	0.387
19	0.077	0.315

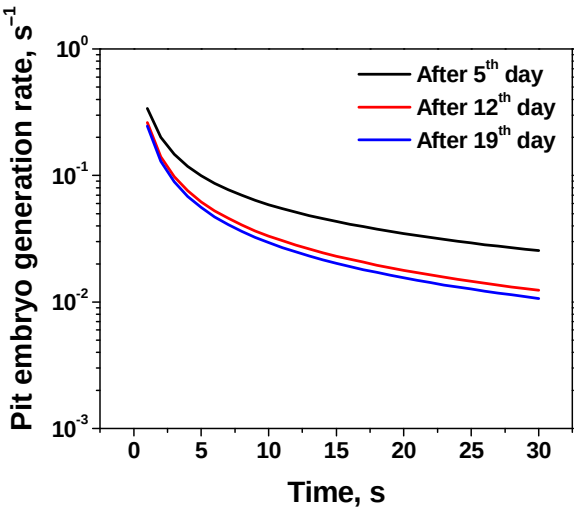

Fig.4 **The pit embryo generation rates for 316LN obtained from Weibull probability plots at different immersion times.**

The pit embryo generation rate was the highest after 5 days exposure and decreased thereafter continuously; with the passage of time, the gap between the pit embryo generation rates shown after 5 days and those shown after 12 and 19 days increases further. Thus, essentially, it can be said that the pit embryo generation rate decreases as a function of exposure time and the generated pit embryos too die faster with the increase in the exposure time.

The cumulative probability of frequency of events, F(f_n) was plotted against the frequency of events, f_n (Fig.5a). Similarly, cumulative probability of characteristic charge F(q) was plotted against

JCSE The Journal of Corrosion Science and Engineering
ISSN 1466-8858 Volume 15, Preprint 8 submitted 18 January 2012

characteristic charge (q) (Fig.5b). It has been reported that the parameters q and f_n derived from shot noise theory provide vital information about the nature of the corrosion processes [15, 19]. Thus, q gives an indication of the mass of the metal lost in the event while f_n provides information about the rate at which these events are happening [14].

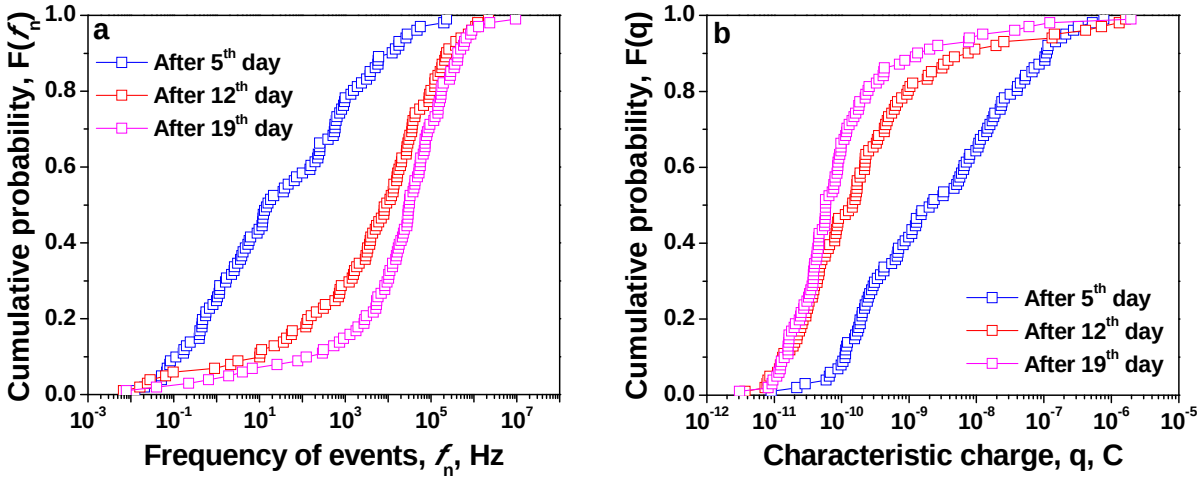

Fig.5 The cumulative probability plots for (a) frequency of events, and (b) characteristic charge; at different time intervals

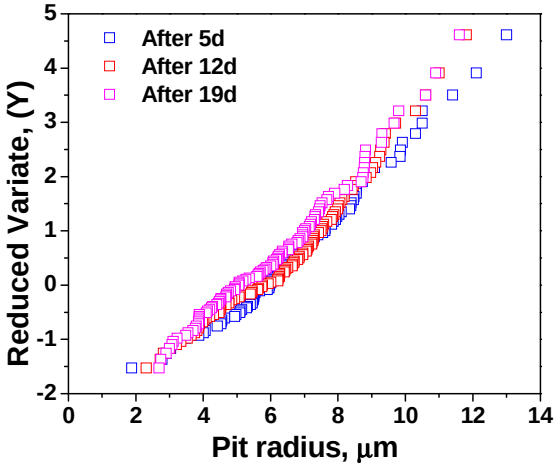

Fig.6 The Gumbel probability plots for 316LN SS at different exposure times in aerated 0.5M sodium chloride solution.

Localized corrosion, such as pitting, can be characterized by a small number of events, and is therefore expected to have a low frequency and high charge [16]. In the case of passivity, the charge is expected to be low, while the frequency will depend on the processes occurring on the passive film [16]. It was reported that the cumulative probability plot in the lower cumulative probability range corresponded to dominant pitting corrosion [13]. Since the pitting corrosion events have the lower cumulative probability, it would be useful in distinguishing the change in the pitting corrosion

JCSE The Journal of Corrosion Science and Engineering
ISSN 1466-8858 Volume 15, Preprint 8 submitted 18 January 2012

resistance of the material as a function of exposure time. At the lowest cumulative probability value, the f_n values appear almost similar at different exposure times; however, as soon as the cumulative probability value increased marginally, a good discrimination was observed and the data obtained after the exposure of five days showed lower frequency of events. Thereafter f_n values increased as a

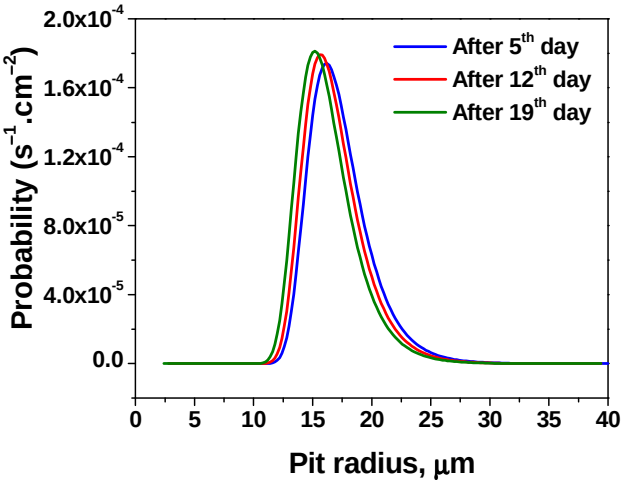

Fig.7 The probability distribution of the metastable pit sizes for at different exposure times for 316LN SS in 0.5M sodium chloride solution.

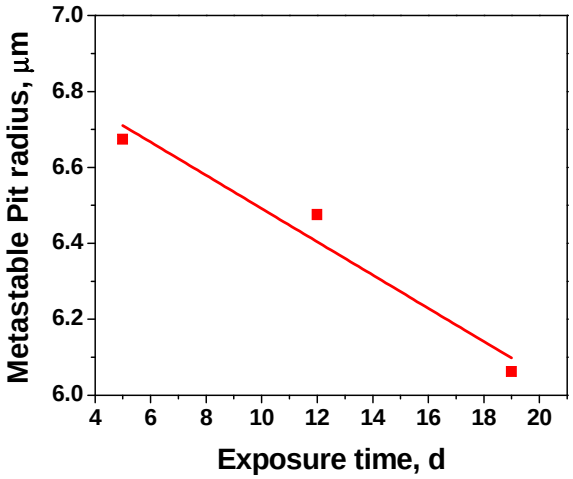

Fig.8 The maximum metastable pit radii as a function of exposure time for 316LN SS in 0.5M sodium chloride solution.

function of exposure time duration at every cumulative probability value signifying decrease in the pitting corrosion tendency of the material. Similarly, it was observed from Fig.5b that at very low cumulative probability value, the q values appeared to be almost same at different exposure times. However, with subsequent increase in the cumulative probability value, the plots got well resolved wherein the plot prepared after 5 days exposure showed high q values. This observation matches with

JCSE The Journal of Corrosion Science and Engineering
ISSN 1466-8858 Volume 15, Preprint 8 submitted 18 January 2012

the one made from the plots in Fig.5a. Thus, metastable pitting corrosion was the highest after 5 days immersion and it slowed down with further exposure.

The plots of the reduced variate (Y) versus the pit radius (μm) are shown in Fig.6. It was observed from Fig.6 that the Gumbel distribution plots for the largest pits in general showed a single slope behavior. Zhang et al. [30, 31] in their studies on Mg alloyed with rare earth elements showed that pit radius versus the reduced variate (Y) plot exhibited two slope behavior which they explained as corresponding to the metastable (relatively smaller pit radii) and the stable pits (relatively larger pit radii) respectively. Thus, the single slope behavior observed in the present studies corresponds to the metastable pits. The values of α, the scale parameter and μ, the location parameter for the distribution of the largest pit were calculated using the data from Fig.6.

The probability distribution of the metastable pit sizes in 0.5M sodium chloride solution is given in Fig.7. The maximum metastable pit sizes are plotted as radii in μm and the probability units are the number of pits per cm^2 per second calculated using equation 11. Figure 8 shows the maximum metastable pit sizes obtained from Fig. 7 as a function of the exposure time. The linear fit of the points in Fig.8 resulted in an equation as follows,

$$Y = A + B*X$$

where, A = 6.93 and B = –0.044. The very small but negative slope in the above equation signifies a continuous decrease in the maximum metastable pit radius as a function of the exposure time. Photomicrographs of the specimens exposed to 0.5M sodium chloride solution for 19 days are presented in Fig. 9 (a, b). These photomicrographs show pit mouths with circular shapes, validating the assumption that the pits are spherical in nature. The measured pit dimensions were found to be much smaller than the metastable pit sizes shown in Fig.6, which truly shows that all the metastable pits do no culminate into stable pits.

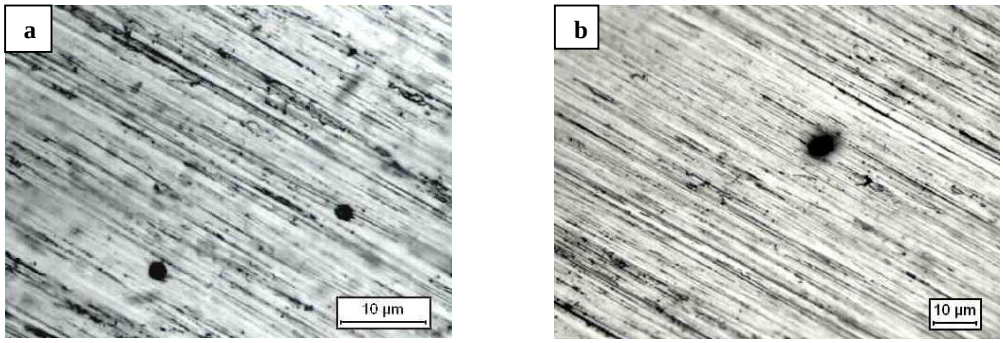

Fig.9 The photomicrographs of the pits (a, b) on 316LN SS exposed to 0.5M sodium chloride solution for 19 days .

In the present investigation, it was noticed that the metastable pits continued to form after adequate time of immersion of the specimen to the sodium chloride solution. However, the conditions for the further growth of the metastable pits into the stable pits were not conducive, thus, these pits eventually ceased to grow. This type of pit growth retarding effect is observed in nitrogen containing stainless steels. A plausible theory suggested that nitrogen in stainless steel will dissolve during corrosion process and consume the acid in pit by a reaction of $[N]+ 4H^+ +3e^- \rightarrow NH_4^+$. This causes a

local neutralizing effect on the acidic environment inside the pits on the corrosion surface, leading to a decreased growth rate of a pit [32, 33]. It was contended by Kamachi et al. [34] that when there was a damage to the passive film the inactive nitrogen layer exposed to the aggressive environment could form inhibiting nitrogen compounds like ammonium ions\nitrate and nitrites through chemical-electrochemical means; these transient short-lived reaction products increase the basicity at the pit surface and reduce the acidic condition necessary for the catalytic pit growth. It has been reported that the passivation properties of the nitrogen added stainless steels were changed advantageously leading to an increased pitting potentials and decreased metastable pitting [35]. The drastic reduction in the metastable pitting events in their experiments was ascribed to the addition of 300 to 400 ppm of nitrogen. In the present work, the nitrogen content in the 316LN SS is 0.067 wt.%, thus it is expected to give a great impetus in arresting the growth of the metastable pits. Pujar et al. [36] observed repassivated pits on 316LN SS during long-term exposure to aerated 0.5M sodium chloride solution, which reinforces the observation that the metastable pits got repassivated. Thus, it was observed that the progress of the metastable pitting is arrested in 316LN SS with continuous exposure to 0.5M sodium chloride solution and this was established by analyzing the EN data using Gumbel distribution function.

Conclusions

The progress of the metastable pitting process in 316LN SS was studied in aerated 0.5M Sodium chloride solution using Weibull and Gumbel distribution functions using EN technique and following were the conclusions of the investigation.

1. Weibull probability plots showed the delay in the initiation of the metastable pitting. Using Weibull distribution function pit embryo generation rates were determined and it was observed that the pit embryo generation rates decreased with increase in the exposure of 316LN to sodium chloride solution. Thus, using pit embryo generation rates, one can determine the metastable pitting corrosion resistance of the alloy under study.
2. Gumbel distribution function showed that the distribution of the pit radii as a function of reduced variate was linear with a single slope indicating that only metastable pits had developed during the exposure. Gumbel distribution function was used to determine the Pit_{max} on 316LN as a function of exposure to sodium chloride solution.
3. The calculated values of Pit_{max} when plotted as a function of time of exposure could be fitted into a straight line with a negative slope; this indicated that the maximum metastable pit radius decreased steadily with time of exposure which was ascribed to the repassivating properties of nitrogen containing stainless steels.
4. The diameters of the pits observed microscopically fall in the range of Pit_{max} values predicted graphically. Therefore, it is possible to predict the pit growth fairly accurately from EN measurements using Gumbel distribution function.

References

1. G. Engelhardt G., D.D. Macdonald, Corrosion Science 46 (2004) 2755.
2. P.C. Pistorius, G.T. Burnstein, Corrosion Science 33 (1992) 1885.
3. G. T. Burnstein, P.C. Pistorius, S.P. Mattin, Corrosion Science 35 (1993) 57.
4. R. Ke and R. Alkire, J. Electrochemical Society 142 (1995) 4056.
5. M.A. Baker, J.E. Castle, Corrosion Science 34 (1993) 667.

ISSN 1466-8858 Volume 15, Preprint 8 submitted 18 January 2012

6. M.P. Ryan, N. J. Laycock, R.C. Newman, H.S. Isaacs, J. Electrochemical Society 145 (1998) 1566.
7. G.S. Frankel, J. Electrochemical Society 145 (1998) 2186.
8. S.T. Pride, J.R. Scully, J.L. Hudson, J. Electrochemical Society 141 (1994) 3028.
9. A.R. Truman, Corrosion Science 47 (2005) 2240.
10. K.-H.Na, S.-I Pyun, Corrosion Science 50 (2008) 248.
11. P.R. Roberge, Electrochemical Noise Measurements for Corrosion Applications, J.R. Kearns, J.R. Scully, P.R. Roberge, D.L. Reichert and J.L.Dawson (eds), ASTM STP 1277, 1996, ASTM, PA, USA
12. R.A. Cottis, Corrosion Science and Engineering 3 (2000) Paper 4.
13. K.-H Na , S.-II Pyun, H.-P Kim, Corrosion Science 49 (2007) 220.
14. J.M. Sanchez-Amaya, R.A. Cottis, F.J. Botana, Corrosion Science 47 (2005) 3280.
15. R.A. Cottis, Corrosion 57 (2001) 265.
16. H. A. A. Al-Mazeedi, R.A. Cottis, Electrochimica Acta 49 (2004) 2787.
17. R.A. Cottis, M. A. A. Al-Awadhi, H. Al-Mazeedi, S. Turgoose, Electrochimica Acta 46 (2001) 3665.
18. A.Valor, F. Caleyo, L. Alfonso, D. Rivas, J.M. Hallen, Corrosion Science 49 (2007) 559.
19. S.-I Pyun and E.-J Lee, Surface and Coating Technology 62 (1993) 480.
20. E.J. Gumbel, *Statistics of Extremes*, Coulombia University Press, New York, (1958).
21. E.J. Gumbel, *Statistical Theory of Extreme Values and Some Practical Application*, National Bureau of Standards, Applied Mathematics Series, No.33, U.S. Government Printing Office, Washington, (1954).
22. P.M. Aziz, Corrosion 12 (1956) 35.
23. T. Shibata, Corrosion 52 (1996) 813.
24. J.E. Strutt, J.R. Nicholis, B. Barbier, Corrosion Science 25 (1985) 305.
25. G.P. Marsh, K.J. Taylor, Corrosion Science 28 (1988) 289.
26. M. Kowaka, (ed). *Introduction to Life Prediction of Industrial Plant Materials: Application of*
27. *the Extreme Value Statistical Method for Corrosion Analysis*, Allerton Press Inc., New York, (1994).
28. K.-H. Na, S.-I Pyun, Journal of Electroanalytical Chemistry 596 (2006) 7.
29. Swapna Dey, Majoj K. Gunjan, Indranil Chattoraj, Corrosion Science 50 (2008) 2895.
30. Tao Zhang, Xiaolan Liu, Yawei Shao, Guozhe Meng, Fuhui Wang, Corrosion Science 50 (2008) 3500.
31. Tao Zhang, Chongmu Chen, Yawei Shao, Guozhe Meng, Fuhui Wang, Xiaogang Li, Chaofang Dong, Electrochimica Acta 53 (2008) 7921.
32. S.D. Chyou., H.C. Shih, Corrosion 47 (1991) 31.
33. H.J. Grabke, International Steel and Iron Journal 36 (1996) 777.
34. U.K. Mudali, B. Reynders, M. Stratmann, Corrosion Science 41 (1999) 179.
35. Lim Yun Soo, Kim Joung Soo, Ahn Se Jin, Kwon Hyuk Sang, Yasuyuki Katada, Corrosion Science 43 (2001) 53.
36. M.G. Pujar, N. Parvathavarthini, S.S. Jena, B.V.R. Tata, R.K. Dayal, H.S. Khatak, Journal of Materials Engineering and Performance 17 (2008) 793.